Active Leg Exoskeleton (ALEX) for Gait Rehabilitation of Motor-Impaired Patients

Sai K. Banala, Suni K. Agrawal and John P. Scholz

Abstract— This paper describes the design and human machine interface of an Active Leg EXoskeleton (ALEX) for gait rehabilitation of patients with walking disabilities. The paper proposes force-field controller which can apply suitable forces on the leg to help it move on a desired trajectory. The interaction forces between the subject and the orthosis are designed to be 'assist-as-needed' for safe and effective gait training. Simulations and experimental results with the force-field controller are presented. Experiments have been performed with healthy subjects walking on a treadmill. It was shown that a healthy subject could be retrained in about 45 minutes with ALEX to walk on a treadmill with a significantly altered gait. In the coming months, this powered orthosis will be used for gait training of stroke patients.

I. INTRODUCTION

Neurological injury, such as hemiparesis from stroke, results in significant muscle weakness or impairment in motor control. Such patients often have substantial limitations in movement. Physical therapy, involving rehabilitation, helps to improve the walking function. Such rehabilitation requires a patient to practice repetitive motion, specifically using the muscles affected by neurological injury. Robotic rehabilitation has many advantages over conventional manual rehabilitation such as: (i) reduced dependence on clinical staff, (ii) interaction forces and torques measured with sensors can assess quantitatively the level of motor recovery, (iii) robotics can help in delivering controlled repetitive training at a reasonable cost.

Currently, available lower extremity orthotic devices can be classified as either passive, where a human subject applies forces to move the leg, or active, where actuators on the device apply forces on the human leg. One of the passive devices is a Gravity balancing leg orthosis (GBO), developed at University of Delaware [1]. This orthosis can alter the level of gravity load acting at a joint by suitable choice of spring parameters on the device. This device was tested on healthy subjects and persons with a stroke to characterize its effect on gait [2].

Passive devices cannot supply energy to the leg, hence are limited in their ability compared to active devices. T-WREX [3] is an upper extremity passive gravity balancing device. Lokomat is an actively powered exoskeleton, designed for

Sai K. Banala: Graduate Student, Mechanical Systems Laboratory, Department of Mechanical Engineering, University of Delaware, Newark, DE 19716,U.S.A. sai@udel.edu

Sunil. K. Agrawal: Professor, Mechanical Systems Laboratory, Department of Mechanical Engineering, University of Delaware, Newark, DE 19716, U.S.A. agrawal@udel.edu

John P. Scholz: Professor, Department of Physical Therapy, University of Delaware, Newark, DE 19716, U.S.A. jpscholz@udel.edu

patients with spinal cord injury. A patient uses this machine while walking on a treadmill [4]. Mechanized Gait Trainer (MGT) is a single degree-of-freedom powered machine that drives the leg to move in a prescribed gait pattern. The machine consists of a foot plate connected to a crank and rocker system. The device simulates the phases of gait, supports the subjects according to their ability, and controls the center of mass in the vertical and horizontal directions [5]. AutoAmbulator is a rehabilitation machine for the leg to assist individuals with stroke and spinal cord injuries. This machine is designed to replicate the pattern of normal gait [6]. HAL is a powered suit for elderly and persons with gait deficiencies [7]. This device takes EMG signals as input and produces appropriate torque to perform the task. Another power-assisted exoskeleton is BLEEX, Berkeley lower extremity exoskeleton [8]. It is not intended to be a rehabilitation device, but a human strength augmenter. PAM, Pelvic Assist Manipulator is an active device for assisting the human pelvis motion [9]. There are a variety of active devices that target a specific disability or weakness in a particular joint of the leg [10], [11], [12], [13].

A limiting feature of some of the motorized exoskeletons used for rehabilitation is that they move a subject through a predetermined movement pattern rather than allowing the subject to move under their own control. The failure to allow patients to self-experience and practice appropriate movement patterns prevents favorable changes in the nervous system for relearning. Cai et-al [14] performed extensive experiments on mice and showed that forced motion along a fixed trajectory may result in "learned helplessness". This is sub-optimal. Instead, 'assist-as-needed' is a better approach. Fixed repetitive training might cause habituation of the sensory inputs and result in the patient not responding well to variations in these patterns. Hence, the interaction force between the human subject and the device plays an important role in training. For effective training, the involvement and participation of a patient in voluntarily movement of the affected limbs is critical. However, at this time, devices which can apply appropriate forces to to the leg during gait rehabilitation, are still in infancy. Another Lower Extremity Powered Exoskeleton (LOPES) [15] has been recently reported. It uses elastic actuators using Bowden cables.

ALEX is shown in Fig. 1 and gait training setup is shown in Fig. 2. The subject walks on a treadmill with orthosis on the right leg. The display in front of the subject provides visual feedback of the executed gait trajectory. The visual display shows the gait trajectory in real time during training. In addition, the subject's performance can be recorded during
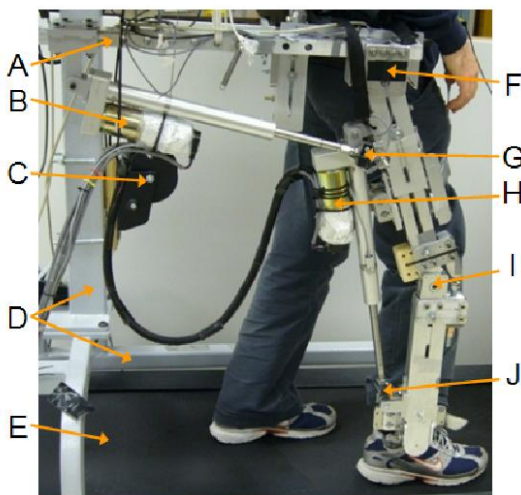
Fig. 1. Powered leg orthosis with a human subject. A: boom to support hip motor, B: hip linear actuator, C: spring-loaded winch to support device weight, D: walker to support the device, E: treadmill F: hip joint, G: load-cell on hip linear-actuator, H: knee linear actuator, I: knee joint J: load-cell on knee linear actuator.
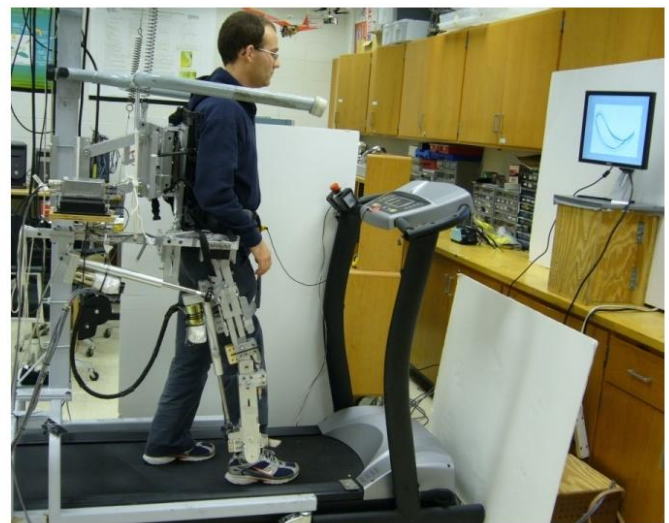

Fig. 2. Gait training exoskeleton on the treadmill, a facility at University of Delaware. The subject walks on a treadmill and the active orthotic device is connected to the right leg. The computer display in front of the subject is for visual feedback of his gait trajectory during training.

each training session. The trajectory can be either joint angles (in joint space) or the foot coordinates (in foot space). This motorized orthosis is architecturally similar to the GBO [1]. A walker with a harness on the trunk keeps the subject stably on the treadmill during exercise. This attachment was found to be quite effective in the performance of GBO and ALEX.

A force-field controller is used to apply desired force fields on the moving leg. The goal of this controller is to assist or resist the motion of the leg, as needed, by applying force-field on the foot. The user is not restricted to a fixed repetitive trajectory. Force-field control uses the concept of assist-force as needed. In other words, force-field controller provides close to zero impedance when the subject moves on the desired gait and offers higher impedance with deviation. This impedance modulation and assistance is achieved by the controller. In contrast with LOPES, ALEX does not use series elastic actuation for backdrivability of the device. Instead, friction compensation is used as described in this paper.

Architecture of force-field controller and simulation results are presented in Section III. Experiments initially performed on a dummy leg for safety are briefly mentioned in Section III-B. Preliminary experiments conducted using ALEX on six healthy subjects and their results are described in detail in Section IV.

II. Orthosis Design

A. Device Description

The design of the active orthosis (Fig. 2) is based on our prototype of passive Gravity Balancing Leg Orthosis [1]. The overall setup has five main components. (i) Walker, which supports the weight of the device. (ii) The trunk of the orthosis, which is connected to a walker and has four degrees-of-freedom (dof). These dof are vertical and lateral translations, rotation about vertical axis and about an axis

perpendicular to sagittal plane. Human trunk is secured to the trunk of the orthosis with a hip brace. (iii) Thigh segment of the orthosis has two dofs with respect to trunk of the orthosis, one in sagittal plane and the other for abduction-adduction motion. The thigh segment is telescopic and can be adjusted to match the thigh length of a human subject. (iv) Shank segment of the orthosis, which has one dof with respect to the thigh segment. Shank segment, like thigh segment, is also telescopic. (v) Foot segment, which is a shoe insert, is attached to the shank of the leg with one dof ankle joint. The foot segment allows inversion-eversion motion to the ankle due to its structural design. All above degrees-of-freedom were found to be essential for achieving natural walking motion of a subject. The hip joint in the sagittal plane and the knee joint are actuated using linear actuators. These motors have encoders built into them, which are used to determine the joint angles. All other degrees-of-freedom are passively held with springs. These motors can generate about 100 Nm peak torques at device knee and hip joints. The physical interface between the orthosis and the dummy/human leg is through two force-torque sensors, one mounted between thigh segments of the orthosis and the leg, the other mounted between shank segments of the orthosis and the leg.

The ankle segment described above is used when a human subject is in the device. During initial testing, we use a dummy leg (Fig. 3), which does not have a foot segment.

B. Safety

As mentioned above, the device is first experimented extensively with a dummy leg which is similar to an average human leg in geometry and inertia distribution. One of the safety feature of the device is physical stops, which are placed on extreme ends of the allowed range of motion of each degree-of-freedom. For hip and knee joints in the sagittal plane which are actuated, the stops can withstand
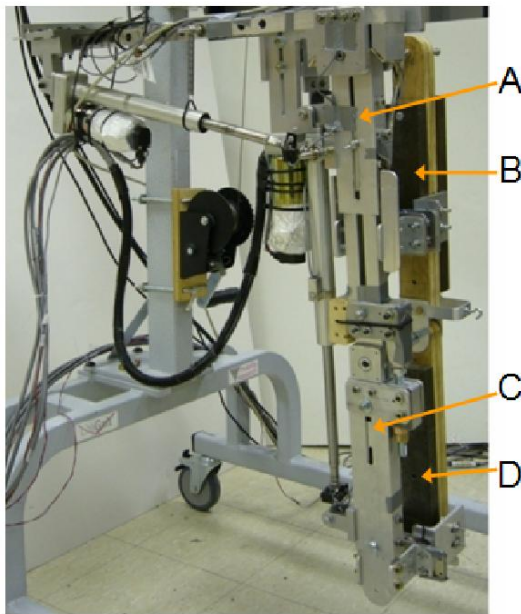
Fig. 3. Powered leg orthosis with a dummy leg. A: device thigh, B: dummy leg thigh, C: device shank, D: dummy leg shank.

the maximum torque the actuators can apply. Two emergency stop switches are wired such that, when activated, can stop both the ALEX and the treadmill. One emergency stop switch is accessible to the subject while the other is given to the personnel overseeing the therapy.

C. Backdrivability of the actuators

To meet the challenging goal of using a light weight motor and at the same time requiring the motor to provide enough torque, we chose a linear actuator driven by an electric motor. These linear actuators cannot be back-driven, i.e., it is very hard to apply force on the linear actuator and drive the motor. This happens because the friction and damping force in the lead screw of the motor gets magnified by its high transmission ratio. However, by using friction compensation, the motor can be made backdrivable. This backdrivability of actuators is important for using force-based control, as it makes it easier for the subject to move their leg without sizable resistance from the device.

The friction compensation methods used are [16]: (1) Model based compensation, in which we feed-forward frictional forces to the controller using a friction model obtained from experiments; (2) Load-cell based compensation, in which we use load-cells in-line with the lead screw of the linear actuator along with a fast PI controller. We have also studied the use of adaptive friction controllers, where we observed that the adaptive identification does not provide good models during external contact [17].

For feed-forward friction compensation, a good friction model is required. Fig. 4 shows the frictional force data collected by experiments conducted on the motor as a function of its linear velocity. The plot has ripples in the first and third quadrants. This behavior can be approximated with
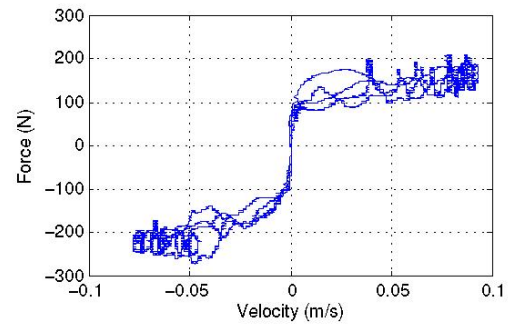

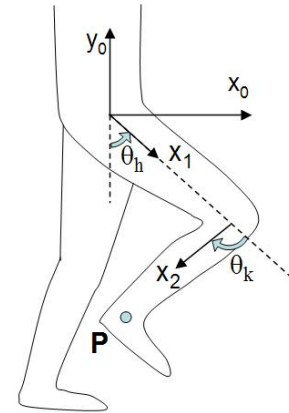Fig. 4. Frictional force in a linear actuator as a function of its linear velocity.

Fig. 5. Schematic showing anatomical joint angle convention.

the equation $F_{friction} = K_{fs} \, \text{sign} \, (\dot{x}) + K_{fd} \dot{x}$, where $\dot{x}$ is the linear velocity of the motor, K_{fs} and K_{fd} are constants.

The friction model is only an approximation and the actual friction has a complicated dependency on the load applied to the motor and on the configuration of the device [18], [19]. Some of the problems of model based friction compensation can be overcome by using a load-cell in series and a fast PI controller with a suitable time constant [17]. Overall, using load-cell based friction compensation along with friction model based compensation gave the best performance.

III. FORCE-FIELD CONTROLLER

The goal of the force-field controller is to create a force field around the foot in addition to providing damping to it. This force field is shaped like a "virtual wall" along the desired trajectory in the sagittal plane. Fig. 6 shows the basic structure of the controller. This controller uses gravity compensation to help the human subject. This assistance can be reduced or completely removed if required. Fig. 7 shows typical shape of a virtual wall around a desired trajectory. It also shows the "width of the tunnel", i.e., the distance to the virtual wall.

Since the virtual walls are used to guide the foot of the subject, the forces are applied on the foot. These forces are a combination of tangential force $\mathbf{F}_t$, normal force $\mathbf{F}_n$ to the desired trajectory and damping force $\mathbf{F}_d$. We designed the controller such that this normal component keeps the foot
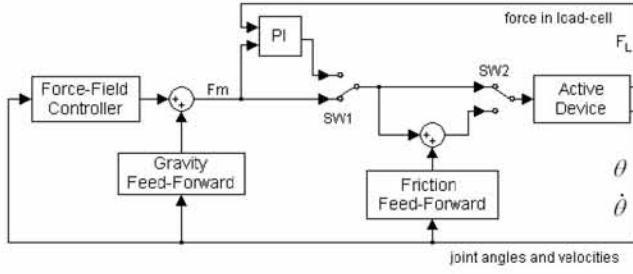
Fig. 6. Force-Field Controller. $\mathbf{F_L}$ is the force measured by the load-cell. Switch SW1 turns on sensor based friction compensation and switch SW2 turns on model based friction compensation.
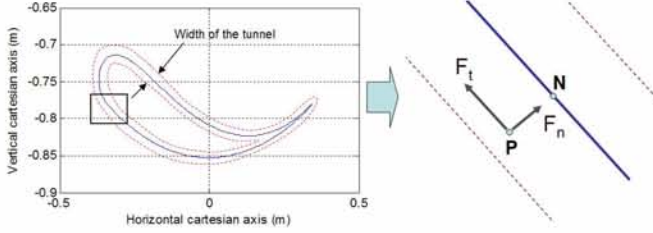

Fig. 7. Cartesian plot of the foot in the trunk reference frame, origin set at the hip joint. The solid line (in blue) is the desired trajectory of the foot and the dashed lines (in red) are the virtual walls.
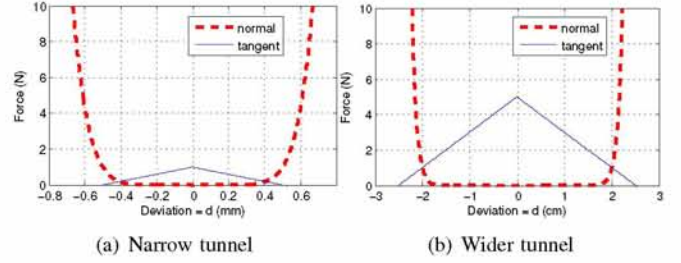

(a) Narrow tunnel   (b) Wider tunnel

Fig. 8. Tangential and normal forces as a function of distance from the desired trajectory, positive force points towards the trajectory. Parameters used are: (a) $K_{Ft} = 1N, D_n = 0.0005m, D_t = 0.0005m, n = 3$, (b) $K_{Ft} = 1N, D_n = 0.02m, D_t = 0.025m, n = 10$
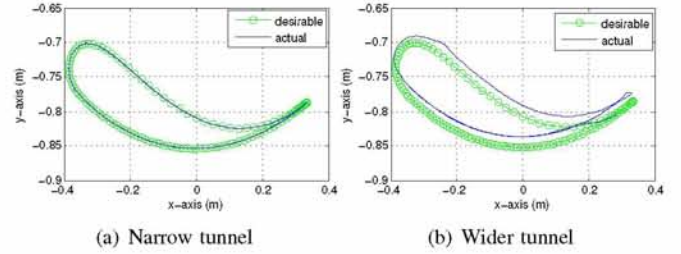

(a) Narrow tunnel   (b) Wider tunnel

Fig. 9. Simulation results of force-field controller showing foot trajectory in Cartesian frame attached to the trunk, origin set at hip joint.

within the virtual tunnel. The tangential force provides the force required to move the foot along the tunnel in forward direction. And the damping force limits the velocities.

Let $\mathbf{P}$ be the current position (Fig. 5 & 7) of the foot in the Cartesian space in the reference frame $(\mathbf{x}_0, \mathbf{y}_0)$ attached to trunk of the subject, $\mathbf{N}$ be the nearest point to $\mathbf{P}$ on the desired trajectory, $\hat{n}$ is the normal vector from $\mathbf{P}$ to $\mathbf{N}$, $\hat{t}$ is the tangential vector at $\mathbf{N}$ along the desired trajectory in forward direction. The force $\mathbf{F}$ on the foot is defined as:

$$\mathbf{F} = \mathbf{F}_t + \mathbf{F}_n + \mathbf{F}_d \qquad (1)$$

where $\mathbf{F}_t$ is the tangential force, $\mathbf{F}_n$ is the normal force and $\mathbf{F}_d$ is the damping force. The tangential force $\mathbf{F}_t$ is defined as:

$$\mathbf{F}_t = \begin{cases} K_{Ft}(1 - d/D_t)\hat{t} & if\ d/D_t < 1 \\ 0 & otherwise \end{cases} \qquad (2)$$

The normal force $\mathbf{F}_n$ is given by:

$$\mathbf{F}_n = \left| \left(\frac{d}{D_n} \right)^n \right| \hat{n}\ . \qquad (3)$$

The damping force $\mathbf{F}_d$ on the foot, to limit velocities, is given by:

$$\mathbf{F}_d = -K_d \dot{\mathbf{x}}\ , \qquad (4)$$

where K_{Ft}, D_t, D_n and K_d are constants, d is the distance between the points $\mathbf{P}$ and $\mathbf{N}$. $\dot{\mathbf{x}}$ is the linear velocity of the foot.

The shape of the tunnel is given by Eq. (3). Higher the value of n, steeper are the walls. Also, at higher values of n,

the width of the tunnel gets closer to D_n. Fig. 8 shows plots of tangential and normal forces as a function of distance d from the desired trajectory, positive force points towards the trajectory. Note that the tangential force ramps down as the distance d increases. This is to bring the leg closer to the trajectory before applying tangential force.

The required actuator inputs at the leg joints that apply the above force field $\mathbf{F}$ is given by:

$$\tau_m = \begin{bmatrix} \tau_{m1} \\ \tau_{m2} \end{bmatrix} = \mathbf{J}^T \mathbf{F} + \mathbf{G}(\boldsymbol{\theta})\ , \qquad (5)$$

where $\mathbf{G}(\boldsymbol{\theta})$ is for gravity compensation. Finally, the forces in the linear actuators $\mathbf{F}_m = [F_{m1}, F_{m2}]$ are computed using the principle of virtual work, given by:

$$\mathbf{F}_{mi} = \frac{\dot{\theta}_i}{l_i} \tau_{mi}, \quad i = 1, 2\ , $$

where l_i is the length of ith linear actuator.

A. Simulations

Simulations were performed using the parameters shown in Fig. 8. We can see in Fig. 9 that with a narrow virtual tunnel, the error in the desired trajectory and the trajectory achieved is smaller when compared to the wider virtual tunnel. This shows that the maximum deviation of the foot from the desired trajectory can be controlled using the width of the tunnel D_n as the parameter. When K_{Ft} is increased from 40 to 60, and all other parameters kept the same ($D_n = 0.02, D_t = 0.025, n = 10$), the tangential force also increases. As a result, the gait cycle period reduced from 5.0 seconds to 3.8 seconds. Thus K_{Ft} can be used as a parameter to change the gait time period.

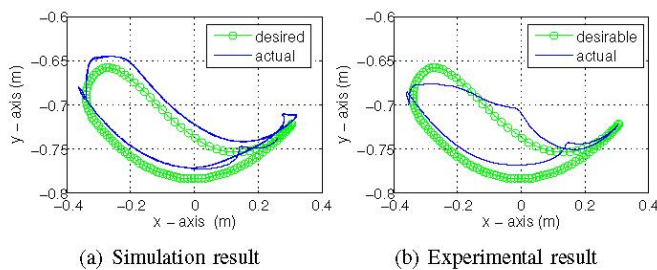(a) Simulation result   (b) Experimental result

Fig. 10. Results of force-field controller showing foot position in cartesian frame attached to the trunk of the subject with origin at the hip joint.

Sl. No.	Sessions	Time (min)	Visual feedback	Force Field		Tunnel width (mm)
				Control group	Expt group	
1	Baseline	5	**OFF**	no	no	-
2	Pre-test	2	on	no	no	-
3	Training - 1	15	on	no	**YES**	3
4	Training - 2	15	on	no	**YES**	6
5	Mid-test	2	on	no	no	-
6	Training - 3	15	on	no	**YES**	6
7	Training - 4	15	on	no	**YES**	8
8	Post-test	2	on	no	no	-
9	Follow up	2	**OFF**	no	no	-

Fig. 11. Details of gait training for subjects in experimental and control groups.

B. Experimental results with dummy leg

The experiments with force field controller were conducted with dummy leg in the device. The parameters used were: $K_{Ft} = 50$N, $D_n = 0.012$m, $D_t = 0.025$m, $n = 3$.

Figure. 10 shows plot of foot trajectory obtained from experiment and through simulation with the same set of parameters ($K_{Ft} = 50, D_n = 0.012, D_t = 0.025, n = 3$). Again, the difference between them could be attributed to the inexact mathematical model used in the simulation. In the figures, one can see the foot bouncing off the virtual tunnel walls.

IV. EXPERIMENTS WITH HEALTHY SUBJECTS

Experiments with the active leg exoskeleton were performed with six healthy adult subjects. This was done to evaluate whether the device could be used to induce short-term adaptations of the walking pattern even of healthy individuals. Note that the subjects also receive visual feedback of their gait trajectory, which could also help in inducing adaptation. To specifically find the effects of the device alone, we used two subject groups: experimental group and control group. A subject in the experimental group is trained with both the active assistance (force-field controller) and the visual feedback. For a subject in the control group, only visual feedback is used. Hence, the difference in adaptation of altered gait pattern in experimental group and control group can be attributed to the force-field control alone.

A. Procedure

Three subjects out of six were assigned to an experimental group who received active assistance from ALEX. This assistance is provided by the force-field controller to produce the sagittal plane foot trajectory during training. As discussed in Section III, force-field controller applies normal force which simulates a virtual wall-like force field around the foot in sagittal plane. Eq. (3) can be used to set virtual wall stiffness so that subjects encounter a non-linear spring-like resistance when the foot path deviates from the prescribed foot path. The tunnel width could be set to allow more (or less) deviation of the current foot path from the prescribed foot path. A significant spring-like resistance was encountered only when the subject reached the "walls" of the tunnel due to the nature of Eq. (3). Tangential force is applied by the controller to assist along the desired foot path. Three

subjects in the control group tried to match a prescribed template without receiving assistance from ALEX.

Figure 11 shows the details of the training procedure for subjects in experimental and control groups. First, the subjects were asked to walk in the device for 5 minutes to get familiarized with it, at this time Force-field and visual feedback are turned off. At the end of this block, subjects "baseline" gait data was recorded. A prescribed foot trajectory was then devised by scaling down each subject's baseline foot path, particularly in the vertical dimension, enough to make replication of the prescribed path challenging. Subjects in both groups received four 15 minute blocks (Training 1 to 4 in Fig. 11) of training trials during which the prescribed template and the subject's current foot path were displayed on a video monitor in front of the subject. Visual feedback was continuous for all training blocks because of limited time to manipulate feedback adequately in these preliminary studies. All four training blocks were identical for the control subjects. For the experimental subjects, both the stiffness of the virtual walls and assisting force were kept constant ($n = 1, K_t = 50$N, $K_d = 30$Ns/m, $D_t = 1$m). What changed was the width of the virtual walls, i.e. the degree of constraint on the foot path. The constraint was maximal for the first block of training trials as the tunnel walls were narrowest ($D_n = 0.003$m). The foot path was less constrained (greater allowable deviation of the foot path from the prescribed path) for blocks 2 and 3 ($D_n = 0.006$m). The constraint of the controller was further reduced during the fourth block of trials ($D_n = 0.008$m). Evaluation of the subjects' walking performance on the treadmill was obtained with the force-field controller turned off (with friction compensation still on) at three time points: (1) prior to the initial block of training (pre-test), (2) prior to block 3 of training (mid-test), and (3) after block 4 of training (post-test). All of these data collections were performed with the template and current foot trajectory displayed to the subject. In addition, following the post-test, video feedback was turned off and the subject's performance was recorded to test for evidence of foot path adaptation or retention (follow up).
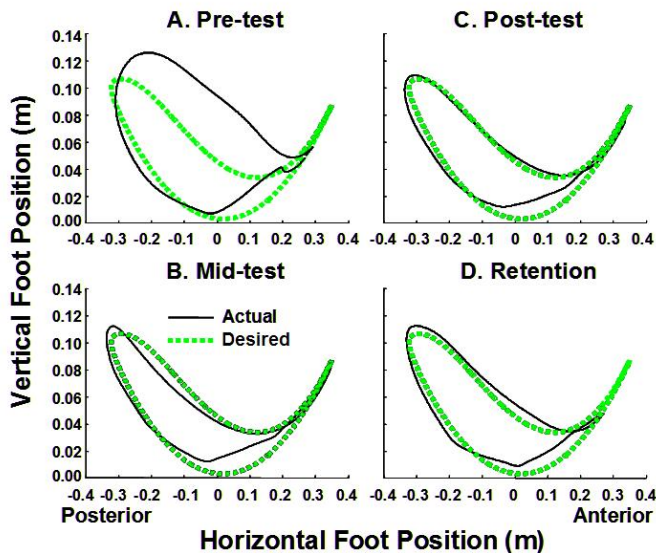
Fig. 12. Plots of sagittal plane foot path of a healthy subject from four evaluation points after training with the ALEX. Although it is shown in the plot for reference, the prescribed trajectory was not shown to the subject during the retention test (bottom, right panel).
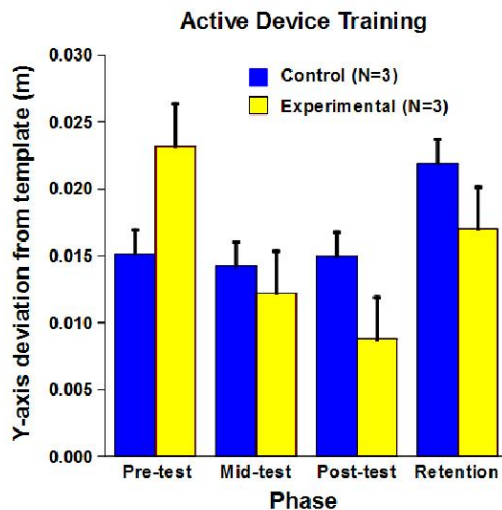

Fig. 13. Average across-subject deviation of vertical foot position from the prescribed template before, mid-way through, and at the end of training with the template displayed to the subject and, finally, with the template turned off (retention).

B. Results

Results of one experimental subject's performance during the four evaluation sessions are illustrated in Fig. 12, where the thin solid line is the subject's average foot path and the heavy dashed line is the prescribed foot path. As shown in the figure, the actual foot path deviated substantially from the required trajectory at the initial evaluation but was shaped to approximate the required trajectory even by the mid-training evaluation. That the trained pattern was maintained reasonably well in this subject following training, after the feedback was turned off completely, is remarkable. Summary results of the vertical deviation of the actual from

the required foot trajectory for all three experimental and control subjects are illustrated in Fig. 13. Only the vertical dimension is illustrated because most of the change occurred in this dimension. Note that the experimental subjects actually had greater foot deviation during the pre-test. The control subjects' performance remained relatively constant throughout, while the experimental group showed a consistent reduction in the deviation from the required trajectory during training. From pre-test to post-test the reduction in deviation for the experimental group is about 60%. This reduction in deviation was partially maintained even after removal of visual feedback, as seen at the retention phase in the figure. This result is striking given that walking patterns are highly ingrained through many years of practice. Of course, interpretation of this result requires caution given that treadmill walking differs significantly from over ground locomotion and is not well-practiced. Nonetheless, the results are encouraging. Our next step is to obtain additional data on healthy subjects using this paradigm and then to evaluate short-term and longer term training of a few patients.

V. Conclusions and Future Work

Powered leg orthosis has been built, following the design of our gravity balancing orthosis (GBO). It has linear actuators at hip and knee joints, it is also instrumented with force-torque sensors and encoders. Force-field controller was developed to provide assistance to the patient. To make the linear actuators back-drivable, these controllers were used with (1) model based and/or (2) load-cell based friction compensation. This backdrivability of the actuators helps the device in making it responsive to the human applied forces by offering least impedance. Simulation and experimental results using force-field controller were presented. Experiments with a dummy leg was done initially and then with six healthy subjects. Among the six subjects, experimental group showed considerable reduction in gait deviation from the prescribed gait pattern when compared to the control group, which shows that there was more adaptation of the walking pattern in experimental group than control group. In the near future, we will use the force-field controller in gait rehabilitation of stroke patients.

VI. Acknowledgments

References

[1] S. K. Banala, S. K. Agrawal, A. Fattah, J. P. Scholz, V. Krishnamoorthy, K. Rudolph, and W.-L. Hsu, "Gravity balancing leg orthosis and its performance evaluation," *IEEE Transactions on Robotics*, vol. 22, no. 6, pp. 1228–1239, dec 2006.

[2] S. K. Agrawal, S. K. Banala, A. Fattah, V. Sangwan, V. Krishnamoorthy, J. P. Scholz, and W.-L. Hsu, "Assessment of motion of a swing leg and gait rehabilitation with a gravity balancing exoskeleton," *to appear in the IEEE Transactions on Neural systems and Rehabilitation Engineering*, 2007.

[3] T. Rahman, W. Sample, and R. Seliktar, "Design and testing of wrex," in *presented at The Eighth International Confrence on Rehabilitation Robotics*, Kaist, Daejeon, Korea, 2003.

[4] G. Colombo, M. Joerg, R. Schreier, and V. Dietz, "Treadmill training of paraplegic patients using a robotic orthosis," *Journal of Rehabilitation Research and Development*, vol. 37, no. 6, 2000.

[5] S. Hesse and D. Uhlenbrock, "A mechanized gait trainer for restoration of gait," *Journal of Rehabilitation Research and Development*, vol. 37, no. 6, 2000.

[6] "Autoambulator," On the WWW, uRL http://www.autoambulator.com.

[7] H. Kawamoto and Y. Sankai, "Power assist system hal-3 for gait disorder person," in *International Conference on Computers for Handicapped Persons*, vol. 2398, 2002, pp. 196–203.

[8] P. Neuhaus and H. Kazerooni, "Design and control of human assisted walking robot," in *the IEEE International Conference on Robotics and Automation*, vol. 1, 2000, pp. 563–569.

[9] D. Aoyagi, W. E. Ichinose, S. J. Harkema, D. J. Reinkensmeyer, and J. E. Bobrow, "An assistive robotic device that can synchronize to the pelvic motion during human gait training," in *IEEE, International Conference on Rehabilitation Robotics*, 2003, pp. 565 – 568.

[10] E. Rocon, A. Ruiz, J. Pons, J. Belda-Lois, and J. S´anchez-Lacuesta, "Rehabilitation robotics: a wearable exo-skeleton for tremor assessment and suppression." in *IEEE, International Conference on Robotics and Automation*, 2005, pp. 2283–2288.

[11] J. Nikitczuk and B. W. andConstantinos Mavroidis, "Rehabilitative knee orthosis driven by electro-rheological fluid based actuators," in *IEEE, International Conference on Robotics and Automation*, 2005, pp. 2294–2300.

[12] G. S. Sawicki, K. E. Gordon, and D. P. Ferris, "Powered lower limb orthoses: applications in motor adaptation and rehabilitation," in *IEEE, International Conference on Rehabilitation Robotics*, 2005, pp. 206 – 211.

[13] C. Acosta-Marquez and D. A. Bradley, "The analysis, design and implementation of a model of an exoskeleton to support mobility," in *IEEE, International Conference on Rehabilitation Robotics*, 2005, pp. 99 – 102.

[14] L. L. Cai, A. J. Fong, Y. Liang, J. Burdick, and V. Edgerton, "Assist-as-needed training paradigms for robotic rehabilitation of spinal cord injuries," in *Proceedings 2006 IEEE International Conference on Robotics and Automation*, 2006, pp. 3504 – 3511.

[15] J. F. Veneman, R. Ekkelenkamp, R. Kruidhof, F. C. T. van der Helm, and H. van der Kooij, "A series elastic- and bowden-cable-based actuation system for use as torque actuator in exoskeleton-type robots," *The International Journal of Robotics Research*, pp. 261–281, 2006.

[16] B. Armstrong-Helouvry, P. Dupont, and C. C. D. Wit, "A survey of models, analysis tools and compensation methods for the control of machines with friction," *Automatica*, vol. 30, no. 7, pp. 1083 – 138, 1994.

[17] J. R. Garretson, W. T. Becker, and S. Dubowsky, "The design of a friction compensation control architecture for a heavy lift precision manipulator in contact with the environment," in *Proceedings 2006 IEEE International Conference on Robotics and Automation*, 2006, pp. 31– 36.

[18] A. Albu-Schaffer, W. Bertleff, B. Rebele, B. Schafer, K. Landzettel, and G. Hirzinger, "Rokviss - robotics component verification on iss current experimental results on parameter identification," in *Proceedings 2006 IEEE International Conference on Robotics and Automation*, 2006, pp. 3879 – 3885.

[19] M. Mahvash and A. M. Okamura, "Friction compensation for a force-feedback telerobotic system," in *Proceedings 2006 IEEE International Conference on Robotics and Automation*, 2006, pp. 3268 – 3273.